

# The Subcellular Organization of Madin–Darby Canine Kidney Cells during the Formation of a Polarized Epithelium

Robert Bacallao,\* Claude Antony, Carlos Dotti, Eric Karsenti, Ernst H. K. Stelzer, and Kai Simons

European Molecular Biology Laboratory, D-6900 Heidelberg, Federal Republic of Germany; and \*Division of Nephrology, University of California at Los Angeles Medical Center, Los Angeles, California 90024

**Abstract.** Studies of the developing trophoderm in the mouse embryo have shown that extensive cellular remodeling occurs during epithelial formation. In this investigation, confocal immunofluorescence microscopy is used to examine the three-dimensional changes in cellular architecture that take place during the polarization of a terminally differentiated epithelial cell line. Madin–Darby canine kidney cells were plated at a low density on permeable filter supports. Antibodies that specifically recognize components of the tight junction, adherens junction, microtubules, centrosomes, and the Golgi complex were used to study the spatial remodeling of the cytoarchitecture during the formation of the polarized cell layer. The immunofluorescence data were correlated with establishment of functional tight junctions as measured by transepithelial resistance and back-exchange of the cell surface, labeled with metabolites of the fluorescent lipid analogue *N*-(7-[4-nitrobenzo-2-oxa-1,3-diazole]) aminocaproyl sphingosine.

1 d after plating, single cells had microtubules, radiating from a broad region, that contained the centro-

somes and the Golgi complex. 2 d after plating, the cells had grown to confluence and had formed functional tight junctions close to the substratum. The centrioles had split and no longer organized the microtubules which were running above and below the nucleus. The Golgi complex had spread around the nucleus. By the fifth day after plating, the final polarized state had been achieved. The junctional complex had moved >10  $\mu\text{m}$  upward from its basal location. The centrioles were together below the apical membrane, and the Golgi complex formed a ribbon-like convoluted structure located in the apical region above the nucleus. The microtubules were organized in an apical web and in longitudinal microtubule bundles in the apical–basal axis of the columnar cell. The longitudinal microtubules were arranged with their minus ends spread over the apical region of the cell and their plus ends toward the basal region. These findings show that there is an extensive remodeling of epithelial cytoarchitecture after formation of cell–cell contacts. Reorganization of the microtubule network results in functional polarization of the cytoplasm.

**T**HE development of cell polarity during epithelialization is a hierarchical process where each cell undergoes a complex sequence of changes in organization before the final polarized state is reached. The decisive event seems to be the establishment of an apical–basal polarity axis. This process is initiated by signals that define the location of the basal pole of the cell through direct interactions with other cells (Fleming and Johnson, 1988) or with the underlying substratum (Hay, 1982; Rodriguez-Boulan et al., 1983; Klein et al., 1988). Subsequently, the apical pole is generated on the opposite side of the cell by little understood alterations of the intracellular organization (Johnson and Maro, 1985; Vega-Salas et al., 1987). The bipolar structure is further modified by lateral interactions between adjacent cells mediated by cell adhesion and junctional proteins (Ducibella and Anderson, 1975; Gumbiner et al., 1988). These protein–protein interactions lead to the formation of circumferential tight junctions that seal the cell layers and divide the

epithelial cell surface into apical and basolateral cell surface domains (Gumbiner, 1987). The maintenance of these two surface domains requires accurate targeting and delivery of newly synthesized plasma membrane components. The Golgi complex plays an important role in this process (Griffiths and Simons, 1986; Wandinger-Ness and Simons, 1989). It is usually positioned above the nucleus in the apical part of the epithelial cell (Cajal, 1914). Newly synthesized apical and basolateral components are sorted in the *trans*-Golgi network into carrier vesicles (Griffiths and Simons, 1986; Bennett et al., 1988). The delivery of these carrier vesicles to the apical plasma membrane seems to be mediated by microtubules (Quaroni et al., 1979; Rindler et al., 1987; Achler et al., 1989; Eilers et al., 1989). One would, therefore, assume that microtubule organization contributes to the development of epithelial polarity. In some cell types, such as fibroblasts, microtubules are organized by the centrosome in the vicinity of the nucleus (Singer and Kupfer, 1986). This

microtubule-organizing complex also affects the localization of the Golgi complex. This interaction is dynamic and involves active movement of Golgi elements towards the minus ends of centrosome-nucleated microtubules (Thyberg and Moskalewski, 1985; Kupfer et al., 1986; Ho et al., 1989). In epithelial cells, microtubule organization is clearly different. The centrioles are located close to the apical surface and do not seem to be major microtubule-nucleating centers (Dustin, 1984; Gorbsky and Borisy, 1985; Bré et al., 1987; Achler et al., 1989). However, the precise organization and the polarity of the microtubules are not known. The relation of microtubule organization to the location of the Golgi complex is also not clear.

In this paper, we have studied the organization of the microtubule network and the Golgi complex when epithelial cells polarize in culture. We have used the Madin-Darby canine kidney (MDCK) strain II cells as our experimental system (Balcarova-Ständer et al., 1984). The cells have been plated on polycarbonate filters and they have been followed from single cells to the fully polarized state. In addition to the Golgi complex and the microtubule network, the formation of lateral cell-cell contacts were studied using an antibody against uvomorulin (E-cadherin), a transmembrane glycoprotein localized to the adherens junctions and along the lateral membranes of adjacent MDCK cells (Boller et al., 1985; Gumbiner and Simons, 1986). The assembly of the tight junctions was analyzed both with the aid of an antibody against the ZO-1 protein (Stevenson et al., 1986) and by an assay that probes the fence function of the junctions (van Meer et al., 1987).

We find that the centrosomes, microtubules, and Golgi complex show a dramatic coordinated reorganization in response to the establishment of cell-cell contacts. In fully polarized cells, microtubules are arranged in vertical bundles with their plus ends facing the basal domain. The Golgi complex is located in the apical-most region of the cell close to the minus ends of the vertical microtubules.

Technically, this study was made possible by the use of confocal beam scanning laser fluorescence microscopy (Stelzer et al., 1989). Immunofluorescence microscopy of labeled specimens using standard epifluorescence microscopy yields images with an unacceptable high background due to endogenous fluorescence from the thick specimen (final height of cell layer was 15–18  $\mu\text{m}$ ) and flare from the filter support. Confocal microscopy offers the advantage of increased resolution and out-of-depth focus discrimination. The digitalized data can be processed for three-dimensional image reconstruction. In this way we could follow the changes in cell architecture occurring during polarization and visualize the complicated organization of the microtubules and the Golgi complex in the final polarized state.

## Materials and Methods

### Fluorescent Probes

Unless otherwise indicated, all fluorescent derivatized second antibodies were obtained from Dianova (Hamburg, FRG). In all cases, the optimal dilution of the secondary antibody for immunostaining was determined on

1. *Abbreviations used in this paper:* C6-NBD-ceramide, *N*-(7-[4-nitrobenzo-2-oxa-1,3-diazole]) aminocaproyl sphingosine; MDCK, Madin-Darby canine kidney; PBS<sup>-</sup>, PBS without Ca<sup>2+</sup> and Mg<sup>2+</sup>.

methanol-fixed MDCK strain II cells. *N*-(7-[4-nitrobenzo-2-oxa-1,3-diazole]) aminocaproyl sphingosine (C6-NBD-ceramide) was obtained from Molecular Probes Inc. (Eugene, OR). Liposomes containing C6-NBD-ceramide were prepared as previously described (Bennett et al., 1988).

### Cell Strain and Culture Conditions

MDCK strain II cells were used for all the studies. The cells were passaged as previously described (Balcarova-Ständer et al., 1984). The cells were grown on polycarbonate filters (Transwell 3412; Costar, Cambridge, MA) with a 0.4- $\mu\text{m}$  pore diameter kindly donated by Hank Lane (Costar). Typically,  $2 \times 10^4$  cells/cm<sup>2</sup> were plated per filter, and the mounted filter was placed in a polypropylene filter support. MEM supplemented with 2 mM glutamine, 5% FCS, 100 U/ml penicillin, and 10  $\mu\text{g}/\text{ml}$  streptomycin was added to the apical and basolateral surfaces of the filters. The cells were incubated at 37°C in a 5% CO<sub>2</sub> hydrated atmosphere.

### Primary Antibodies

Affinity-purified rabbit anti-tubulin was generously provided by Jan De Mey (European Molecular Biology Laboratory, Heidelberg, FRG). Anti-ZO-1 was a generous gift from Bruce Stevenson (Yale University, New Haven, CT). M3A5 is a monoclonal antibody that recognizes a peripheral membrane protein of the Golgi complex and it was used to follow the changes in Golgi morphology (Allan and Kreis, 1986). Uvomorulin staining was performed using the monoclonal antibody rrl (Gumbiner and Simons, 1986). The monoclonal antibody 45H3, obtained by immunization of mice with purified human centrosomes, was generously provided by Michel Bornens (Gif-Sur-Yvette, France) (Bornens et al., 1987).

### Measurement of the Transepithelial Resistance

Measurement of the transepithelial resistance was performed as previously described (Gumbiner and Simons, 1986). The transepithelial resistance was measured on the filter-grown cells on days 1–5 after plating. After the resistance was measured, the filters were placed back in the growth media and incubated for 1 h in the incubator before fixation.

### Fixation Methodology

Cells that were stained for the centrioles and ZO-1 were fixed by dipping the filter in PBS with 1 mM Ca<sup>2+</sup> and 0.5 mM Mg<sup>2+</sup> warmed to 37°C. The filters were quickly blotted on Whatman filter paper to remove excess moisture and dipped for 1 min in a bath containing -20°C methanol. The filter was transferred to a fresh bath of -20°C methanol. The cells were washed in PBS without Ca<sup>2+</sup> and Mg<sup>2+</sup> (PBS<sup>-</sup>) followed by a wash with PBS<sup>-</sup>, 0.1% Triton X-100.

Except for the centrosome and ZO-1 staining, all the cells were fixed by a modification of the paraformaldehyde fixation described by Berod et al. (1981). The filter was dipped in 80 mM K-Pipes, pH 6.8, 5 mM EGTA, 2 mM MgCl<sub>2</sub> warmed to 37°C. The cells were incubated in 3% paraformaldehyde, 80 mM K-Pipes, pH 6.5, 5 mM EGTA, 2 mM MgCl<sub>2</sub> for 5 min at room temperature. This solution was added to both the apical and basal compartments of the filter holder. The solution was removed and the cells were fixed with 3% paraformaldehyde (Merck GmbH, Darmstadt, FRG), 100 mM NaB<sub>4</sub>O<sub>7</sub>, pH 11. The cells were incubated in this fixation solution for 10 min under continuous agitation at room temperature. The reaction was quenched by incubating the filters in 1 mg/ml NaBH<sub>4</sub> freshly dissolved in PBS<sup>-</sup>, pH 8, for 10 min. The pH of the PBS was brought up to 8 with 6 N NaOH to increase the half-life of the NaBH<sub>4</sub> in solution. The repeated treatments of the specimens with NaBH<sub>4</sub> resulted in a significant decrease in endogenous background fluorescence. The cells were washed three times in PBS<sup>-</sup>, pH 7.4, and the specimen was permeabilized with PBS<sup>-</sup>, 0.1% Triton X-100. Those samples that were fixed to stain for the centrosomes, in combination with microtubule or Golgi staining, were dipped in -20°C methanol for 5 s before the quenching reaction. These samples were not treated with Triton X-100.

### Immunostaining

The filters were cut from the plastic support holders and were divided into four squares. Each filter square was washed twice in PBS<sup>-</sup>, 0.2% fish skin gelatin (Sigma Chemie GmbH, Deisenhofen, FRG), 0.01% NaN<sub>3</sub>, 0.1% Triton X-100. This solution was used to dilute all the antibodies used in this paper. Unless otherwise stated, each wash entailed an incubation on a shak-

ing table for 15 min at room temperature. 60  $\mu$ l of antibody solution was placed on parafilm, and the filter squares were placed cell side down on the antibody solution. The specimens were incubated in a humidified chamber at 37°C for 45 min. The filter squares were removed, placed on a fresh aliquot of antibody solution, and incubated for an additional 45 min. After the antibody incubation steps, the filters were washed twice in PBS-, 0.2% fish skin gelatin, 0.01% NaN<sub>3</sub>, 0.1% Triton X-100. This was followed by three washes in PBS-, 0.01% NaN<sub>3</sub>, 0.1% Triton X-100. After the washes following the primary antibody incubation, the filter was washed once again in PBS-, 0.2% fish skin gelatin, 0.01% NaN<sub>3</sub>, 0.1% Triton X-100 before the second antibody incubation. In the washes after the second antibody incubation, the three washes were followed by three 5-min washes in PBS-.

The labeled cells were postfixed in 4% paraformaldehyde in 50 mM Na-cacodylate, pH 7.5, buffer for 30 min at room temperature. This reaction was quenched with 50 mM NH<sub>4</sub>Cl dissolved in PBS for 45 min. The filters were washed in PBS- three times for 5 min and then stored at 4°C in PBS-, 0.01% NaN<sub>3</sub> until examined with the confocal microscope.

The specimens made for analysis with the confocal scanning laser beam fluorescence microscope were mounted on glass slides with four spacers made with acrylic nail polish. A drop of 50% glycerol, PBS- with 100 mg/ml 1,4 diazabicyclo-(2.2.2) octane (Sigma Chemie GmbH) was placed on the cell side of the filter, and a glass coverslip was carefully lowered onto the spacer supports. This ensured that the coverslip did not compress the sample. The mount was sealed on three sides with acrylic nail polish. 1,4 Diazabicyclo-(2.2.2) octane was used as an anti-bleaching agent.

### *In Vivo Labeling Using C6-NBD-Ceramide*

The cells were labeled with C6-NBD-ceramide as previously described with the exception that 13 nM C6-NBD-ceramide was used for labeling instead of 26 nM (van Meer et al., 1987). The cells were labeled at 37°C. Back-exchange of the fluorescent probe was performed with 1% BSA in Hanks' basic salts solution with 10 mM Na-Hepes buffer, pH 7.5, at 10°C for a total of 30 min. The first incubation was performed for 10 min, and the medium was replaced with a fresh aliquot of back-exchange medium.

### *Fluorescence Microscopy*

Epifluorescence microscopy was performed on a microscope (Axioptot; Carl Zeiss, Inc., Thornwood, NY) equipped for standard epifluorescence microscopy. Photographs were taken with Tmax P3200 film (Eastman Kodak Co., Rochester, NY). Confocal fluorescence microscopy was performed with the confocal scanning laser beam fluorescence microscope developed at the European Molecular Biology Laboratory. A description of the design and operating principles of the confocal fluorescence microscope at the European Molecular Biology Laboratory has been published previously (Stelzer et al., 1989). Two wavelengths (476 and 514.5  $\mu$ m) out of several lines produced by an argon laser (2020-05; Spectra-Physics Inc., Mountain View, CA) were used to excite FITC and Texas red, respectively.

### *Image Acquisition and Processing*

Samples were analyzed with the confocal scanning laser fluorescent microscope within 1 wk after fixation and staining. Prior experiments showed there was no loss of three-dimensional information when the specimens were stored as described above. Images of serial optical sections, 0.4 cm thick, were stored in a microcomputer (VME H68010; Eltec, Mainz, FRG). One image was comprised of 512 by 512 pixels. Stereo pair images were computed from the data set. The images were photographed using a black and white monitor (Knott elektronik, Hoenschaftlan, FRG) and a pre-focused camera. Tmax ASA 100 film (Eastman Kodak Co.) was used in all the photographs obtained on line. Some of the images were generated using a workstation (VAX 3200; Digital Equipment Corp., Nashua, NH) and a modified version of the View image processing program kindly provided by Lawrence Livermore Laboratory (Livermore, CA). Images generated from the workstation (VAX 3200; Digital Equipment Corp.) were photographed with daylight Ektachrome plus (ASA 100) film (Eastman Kodak Co.).

### *Viewing the Stereo Images*

The stereo images presented in this paper are preferably viewed with stereoscopes or stereoglasses. Fig. 8 should be viewed with stereo glasses. The other stereo images were viewed using a reflecting stereoscope. These are distributed by VCH Publishers (22 E. 23rd St., New York, NY 10010). In Europe the stereoscopes may be ordered from VCH Verlagsgesellschaft

(P.O. Box 12 60/12 80, D-6940 Weinheim, FRG). Stereo glasses can be obtained from Hubbard Scientific (Northbrook, IL).

### *Determination of the Polarity of Microtubules*

The microtubule polarity was determined by the "hook" method modified for filter-cultured MDCK cells (Heidemann and McIntosh, 1980). This method relies on the ability of exogenous tubulin in a high ionic strength buffer to polymerize in the form of lateral sheets along the walls of existing microtubules. The lateral sheets of the newly formed microtubules then appear as hooks in cross sections. A clockwise hook indicates that the "plus" end of a microtubule is directed towards the observer. A counterclockwise hook indicates the opposite. For this paper, all sections were made parallel to the filter starting from the cell basal surface to analyze the polarity of vertically running microtubules. Thus, the observer always looks at the cells from the perspective of the basal surface.

Bovine brain tubulin was purified by the method described by Mitchison and Kirschner (1984). Bovine brain tubulin, 2 mg/ml, was added to MDCK cells in the following way. The apical surface was lysed with 2 ml of "lysing polymerizing" buffer (0.5 M K-Pipes, pH 6.8, 10 mM MgCl<sub>2</sub>, 20 mM EGTA, 0.1 mM GTP, 20% glycerol, 2.5% DMSO, 0.125% Triton X-100, 2 mg/ml tubulin) applied to the apical side of the filter for 5 min at 37°C. The buffer was removed and replaced by the same buffer without detergent. The cells were incubated for 1 h at 37°C. At the end of the incubation, the filters were carefully rinsed with 0.5 M K-Pipes, pH 6.8, 10 mM MgCl<sub>2</sub>, 20 mM EGTA, 0.1 mM GTP, 20% glycerol, 2.5% DMSO, immediately dipped in 4% glutaraldehyde in 100 mM Na-cacodylate buffer warmed to 37°C for 3 min, and rinsed and further fixed for 30 min in 2% glutaraldehyde. Excess fixative was removed by several washes in cacodylate buffer. The filters were incubated in 0.4% tannic acid for 5 min and postfixed for 2 h in 2% osmium tetroxide. The monolayers were rinsed in water and stained en bloc with 0.5% uranyl acetate at 4°C for 12 h. The sample was dehydrated by serially incubating the sample in 40% ethanol followed by solutions containing increasing amounts of ethanol until a 100% solution of ethanol was used. The filters were processed for conventional embedding in Epon by placing the filter, cell side down, onto a plastic capsule previously filled with Epon. A glass coverslip was placed on the top to flatten the filter during polymerization. After removing the coverslip by dipping the blocs in liquid nitrogen, the monolayers were cut parallel to the basal side, starting from the filter side towards the apical region of the cells. These sections were used to examine the polarity of the vertically running microtubules. The polarity of microtubules running perpendicular to the apical-basal axis was examined in sections cut perpendicular to the filter surface. After sectioning, contrast was increased by 15 min of staining in 3% uranyl acetate in 50% ethanol followed by a lead citrate staining for 1 min. Pictures were taken at 60 kV on an electron microscope (301; Philips Electronic Instruments, Inc., Mahwah, NJ).

A different approach to incorporate exogenous tubulin without producing extensive damage of the cell membrane organization was by cell electroporation. The electroporation system consisted of two round, 1.5-mm-thick stainless steel electrodes connected to a high-voltage power supply (built by W. Ansoerg's group at the European Molecular Biology Laboratory). The apical electrode and the basal electrode had diameters of 22 and 30 mm, respectively. An exponentially decaying current of 700 V/cm<sup>2</sup> was applied in five pulses of 100  $\mu$ s duration. The apical electrode was suspended 0.8 mm above the filter to achieve a reproducible percentage of electroporated cells. Polymerizing buffer, without detergent, was put above the apical cell surface and the current was applied. The electrodes were removed and the cells were incubated in polymerizing buffer for 1 h at 37°C. At the end of the incubation, the cells were fixed and processed as above.

### *Results*

#### *Microtubule Remodeling during the Formation of a Columnar Epithelial Cell Monolayer*

1 d after plating, all the cells had spread upon the filter support. Most of the cells were isolated and had a flattened cytoplasmic region. The nucleus was centrally located, and the maximal height of the cells was 4–6  $\mu$ m at the level of the nucleus (Fig. 1 A). This height corresponded to the approximate diameter of the nucleus. The predominant pattern of

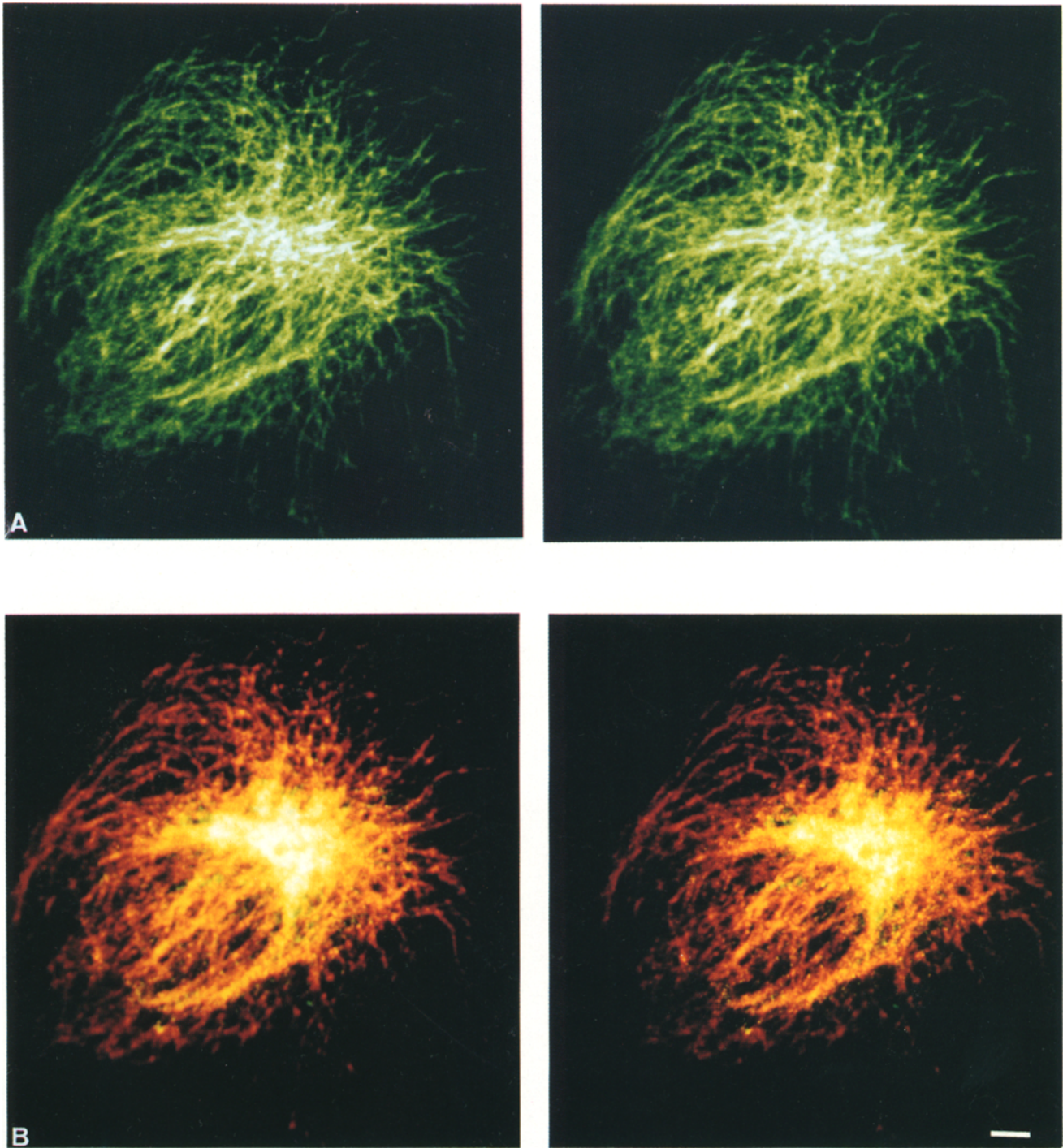


**Figure 1.** Stereo pair images of microtubules and the Golgi complex in an isolated MDCK cell 1 d after plating. The microtubules were stained with a combination of rabbit anti-tubulin and FITC-conjugated goat anti-rabbit IgG antibodies. The Golgi complex was stained with the mouse monoclonal antibody (M3A5) and Texas red-derivatized goat anti-mouse IgG antibodies. The image was acquired separately for each wavelength, and the data set was stored in the Vax 3200 computer (Digital Equipment Corp.). Each stereo image is composed of the superimposition of a series of  $512 \times 512$  pixel images in the *x*- and *y*-plane separated by  $0.4 \mu\text{m}$  along the *z*-axis. Each image was generated using a pseudocolor scale. The stereo images of the microtubules and Golgi complex were generated separately and then mapped onto each other using the View image processing program. (A) Microtubule staining; (B) double labeling of the microtubules and Golgi complex. The microtubule image was mapped with a red colorscale, while the Golgi complex image was generated with a green colorscale. Bar,  $5 \mu\text{m}$ .

microtubule organization is shown in Fig. 1 A. Note that many microtubules originated from a broad region eccentrically placed near the nucleus. This pattern, which seems to be generated by a single microtubule-organizing complex

(Kronebusch and Singer, 1987), was found in 86% of the cells examined (Tables I and II). In these cells, the two centrioles were close to each other, near the nucleus, and localized in the region from where microtubules originated. In other

**Table I. Centrosome Colocalization with a Single Microtubule-organizing Complex**

MTOC*	Cells	Centrioles together and colocalized with MTOC	Centrioles split	Centrioles together and did not colocalize
	<i>n</i> (%)	<i>n</i> (%)	<i>n</i> (%)	<i>n</i> (%)
Present	86 (86)	72 (84)	—	14 (16)
Absent	14 (14)	—	10 (71)	4 (29)

Cells were fixed and stained as described in Materials and Methods. The centrioles were stained with Texas red-derivatized goat anti-mouse IgG. The microtubules were stained with FITC-conjugated goat anti-rabbit IgG. The cells were examined using an epifluorescence microscope.

\* Single microtubule-organizing complex.

cells (14% of the population), the microtubules had no single nucleating center, and the centrioles were found separated from each other in variable locations (Tables I and II).

2 d after plating, the cells established intercellular contacts, and a transepithelial resistance, ranging between 20 and 40  $\Omega \cdot \text{cm}^2$  developed. The long axis of the cell was still parallel to the substratum, and the height of the cells varied between 6 and 10  $\mu\text{m}$  at the level of the nucleus. Although in some cells microtubules were still originating from a localized perinuclear region (Fig. 2 A, arrow), in most cases they formed a crisscrossed apical network and did not appear to originate from a single nucleating center (Fig. 2, A and B). The stereo images gave the impression that microtubules were rearranging parallel to the long axis of the cell below the apical plasma membrane. Removal of the apical cap by the computer showed that microtubules were also present below the nucleus parallel to the basal plasma membrane (Fig. 2 C).

On the fifth day of growth, the cells were columnar, 15–18  $\mu\text{m}$  high. Stereo images showed a complex microtubule pattern with the presence of cilia (Roth et al., 1988) in almost all of the cells (Fig. 3 A). Inside the cells, the microtubule staining pattern appeared as dots or fibers parallel to the apical–basal axis. Most microtubules did not seem to radiate from the centriolar region, conveniently marked by the cilium.

Because of the density of the apical staining, it was difficult to see how microtubules were organized in the basal parts of the cell. To gain visual access to this region, the first seven (apical) optical sections (2.8  $\mu\text{m}$ ) were removed by the computer and the stereo image was regenerated from the remain-

**Table II. Golgi Morphology and Colocalization with a Single Microtubule-organizing Complex**

MTOC*	Cells	Golgi morphology		
		Contracted	Spread	Indeterminate
	<i>n</i> (%)	<i>n</i> (%)	<i>n</i> (%)	<i>n</i> (%)
Present	89 (85)	84 (94)	1 (1.1)	4 (4.6)
Absent	16 (15)	—	16 (100)	—

Cells were fixed and stained as described in Materials and Methods. The Golgi complex was stained with a Texas red-derivatized goat anti-mouse IgG. The microtubules were stained with FITC-conjugated goat anti-rabbit IgG. The cells were examined using an epifluorescence microscope.

\* Single microtubule-organizing complex.

ing optical sections (Fig. 3 B). The part of the figure closest to the observer corresponded to the region just above the nucleus. The microtubule bundles are running down along the cell borders and splay into the basal domain where they form a sparse network in most cells.

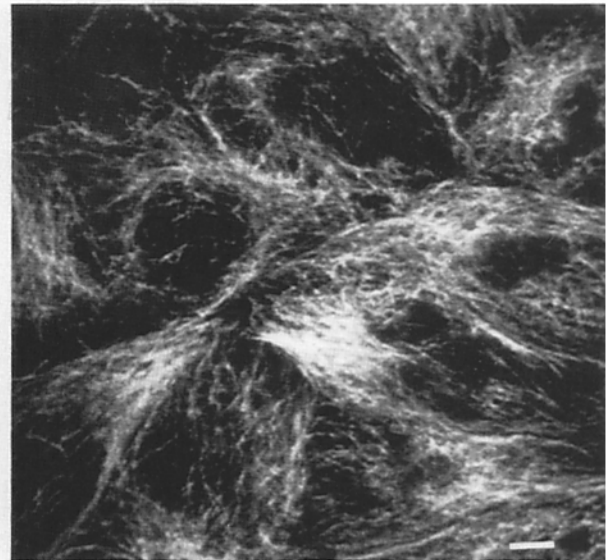
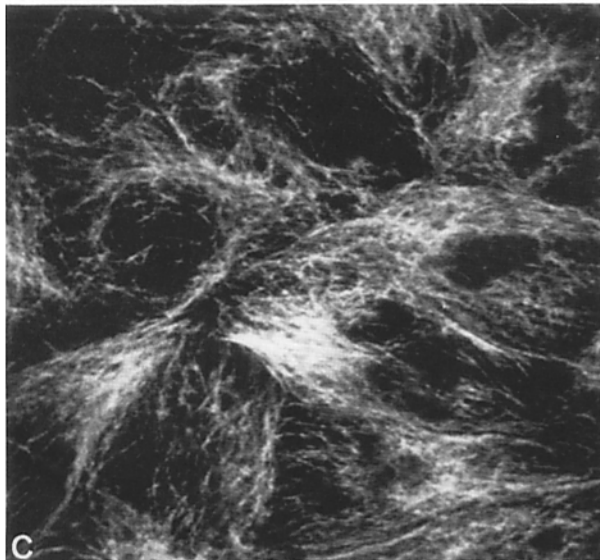
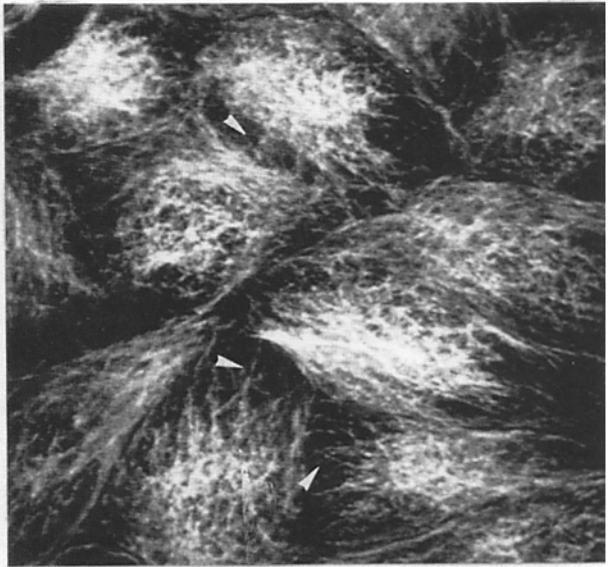
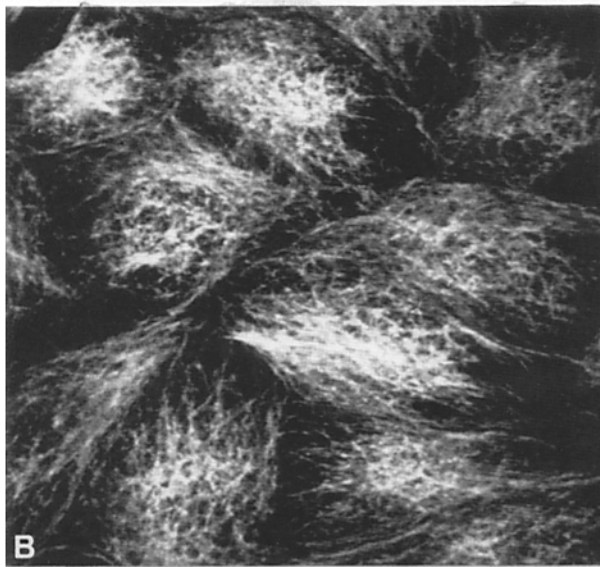
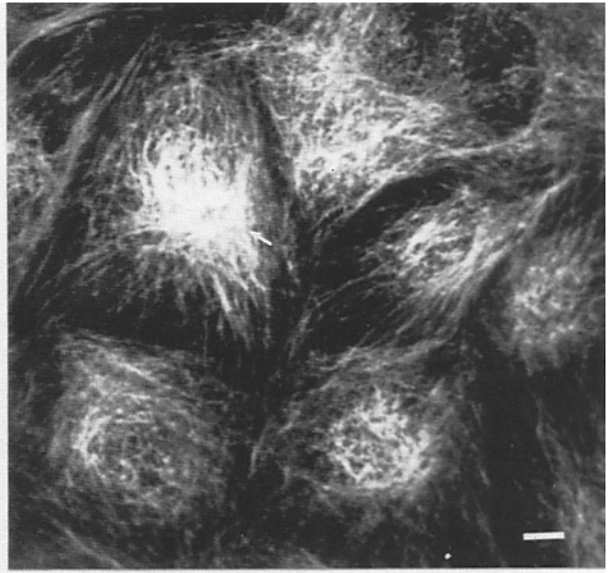
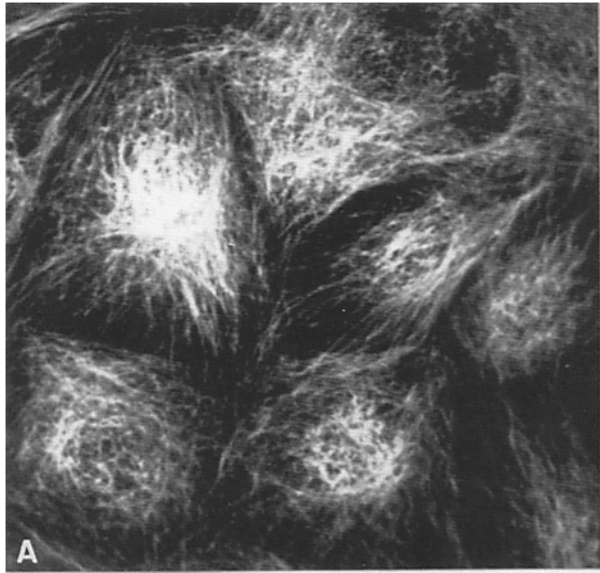
Three of the horizontal sections that were used to generate the stereo images in Fig. 3, A and B, are shown in Fig. 4. They highlight the predominant features of microtubule organization in the final differentiated state. In the apical domain, 0.4  $\mu\text{m}$  below the base of the cilium (Fig. 4 A), the tubulin staining revealed dots or short segments. 8  $\mu\text{m}$  deeper into the cell, the tubulin staining was found in thick perinuclear dots probably deriving from apical–basal bundles of microtubules (see below). Finally, in the basal domain a sparse microtubule network was seen.

### Microtubule Polarity

The polarity of the longitudinal microtubules was determined by the hook procedure (Heideman and McIntosh, 1980). In the first series of experiments the polarity of the microtubules running vertically between the apical and basal domains was determined by sectioning the cells parallel to the filter plane. An example of microtubule decoration by tubulin after permeabilization with Triton X-100 is shown in Fig. 5, A and B. Four out of five microtubules found in this section showed right-handed hooks. The fifth microtubule (Fig. 5 A) exhibited an equivocal orientation. A similar pattern was observed throughout the entire central region of the cells. As shown in Table III, 90% of the decorated microtubules had hooks with a clockwise orientation. This means that microtubules have their plus end directed mostly toward the basal domain. The same orientation of the microtubules was uniformly observed in sections cut close to the apical and basal cell surfaces. The vertical microtubules were often arranged in bundles running either along the cell boundaries or close to the nuclear envelope. This was found by electron microscopy of both untreated and detergent-extracted cells (data not shown).

The polarity of microtubules arranged along the apical–basal axis of the cells was also determined in the apical–most domain. As shown in Fig. 6, A and B, and Table III, 85% of the decorated microtubules had clockwise hooks, even in the apical–most region of the cells. Because detergent extraction altered the ultrastructure of the apical region, this analysis was repeated using electroporation to introduce tubulin into the cells. With this procedure, the overall intracellular organization, membrane and organelle integrity, was significantly better preserved than with detergent treatment (Fig. 6 C); we found the same polarity of apical–most microtubules as after detergent extraction. However, these microtubules were not usually bundled.

Some microtubules in the apical domain did not run along the apical–basal axis but were parallel to the apical membrane. Since the apical microtubules did not appear to have a single organizing center, it was of interest to determine whether or not, in a given section, these microtubules all had the same polarity. If the microtubules were originating from several sites, the prediction would be that the microtubules should have different polarities. For this analysis, blocks were sectioned perpendicular to the filter— i.e., parallel to the apical–basal axis. The decorated microtubules cut trans-



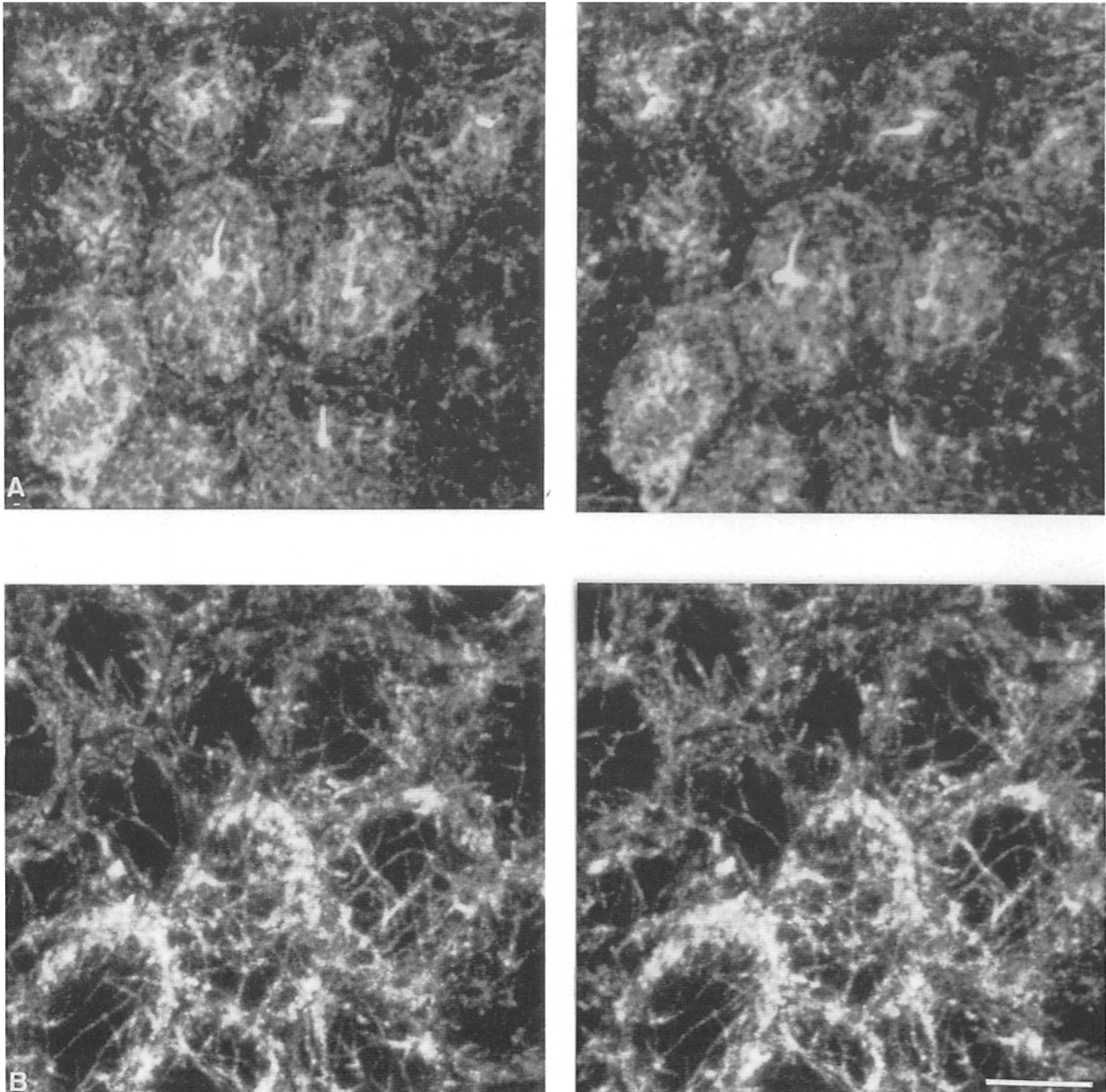


**Figure 3.** Stereo pair images of microtubule staining in MDCK cells 5 d after plating. (A) The cells have formed a columnar epithelium with protruding cilia. There are many “dot-like” structures seen in the apical part of the cell with short but thick fibers running between the dots. Microtubule bundles run along the apical–basal axis of the cells. (B) The first seven apical optical sections have been removed (Fig. 2 B), corresponding to a distance of 2.8  $\mu\text{m}$ , and the resulting image begins 1.2  $\mu\text{m}$  above the nucleus. The total height of the cells is  $\sim 14 \mu\text{m}$ . The longitudinal bundles and the basal network are now more easily seen. Bar, 5  $\mu\text{m}$ .

versely showed hooks with the clockwise and counterclockwise orientation in equal proportions (Fig. 7). This mixed polarity suggested that there was no unique microtubule-nucleating center in the apical region of polarized cells.

#### ***Golgi Complex Relocation during the Formation of a Columnar Epithelial Cell Monolayer***

The dramatic change in microtubule organization observed during the establishment of polarity in MDCK cells led us

**Figure 2.** Stereo pair images of microtubule staining in MDCK cells 2 and 3 d after plating. (A) Occasional cells maintain the perinuclear microtubule-organizing complex 2 d after plating (arrow). (B) 3 d after plating, most of the cells have diffusely organized microtubules in the apical region forming a crisscross pattern. Peripherally, the microtubule pattern is sparse (arrowheads). (C) Cutaway view of B. The first six images are removed from this image and the stereo image is regenerated from the remaining images. This removes the apical network and allows visualization of the underlying microtubule organization. Bar, 5  $\mu\text{m}$ .

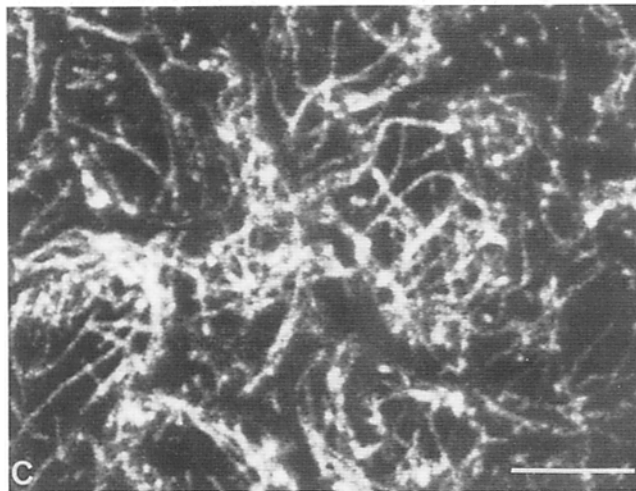
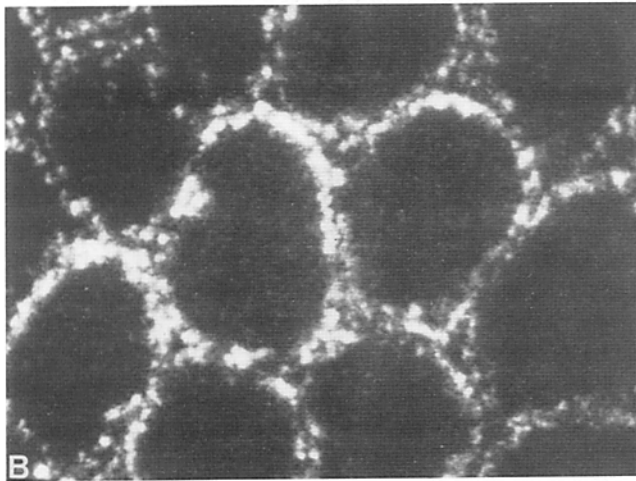
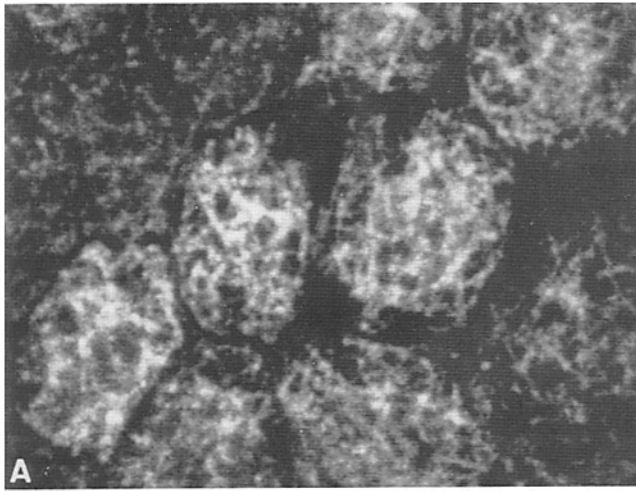


**Figure 4.** Microtubule staining in three optical sections of columnar MDCK cells shown in Fig. 3. (A) Section through the upper apical region. A punctate pattern with short thick connecting segments of microtubules can be seen. (B) Optical section through the nuclear region. Note the thick dots, which are composed of microtubule bundles that are perpendicular to the image plane. (C) Section through the basal region of the cell. Microtubules run parallel to the basal membrane. In addition, dots are seen at this level which derive from microtubules that are perpendicular to the membrane surface. Bar, 5  $\mu\text{m}$ .

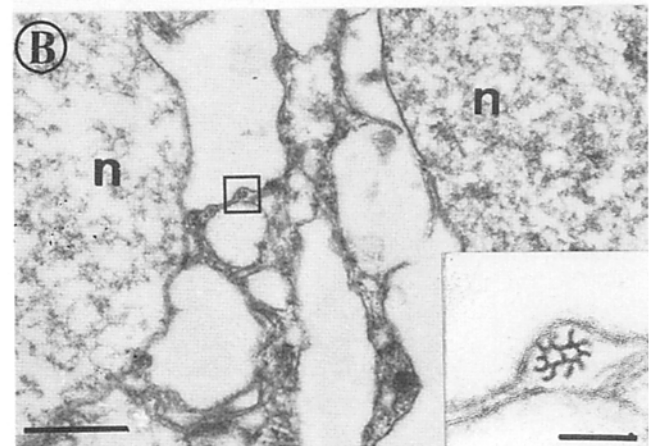
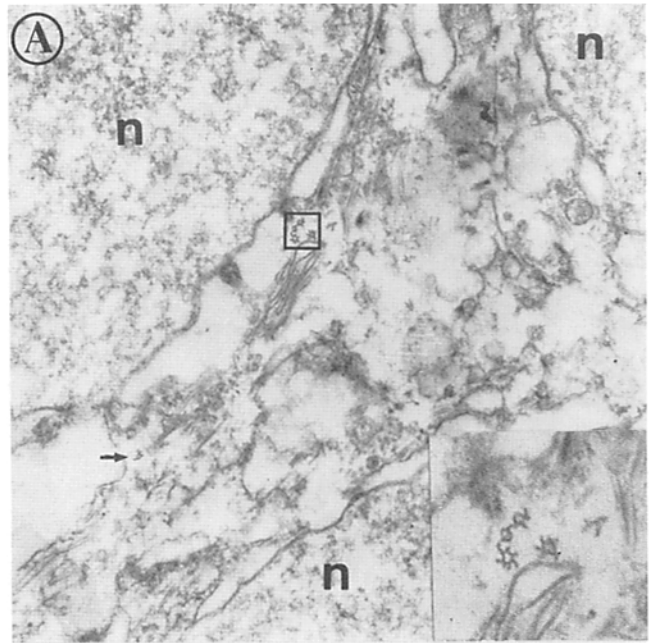


**Figure 5.** Polarity of the microtubule bundles in the perinuclear region of MDCK cells 5 d after plating. The cells were permeabilized with Triton X-100 and incubated with tubulin. (A) Horizontal section through the nuclear region of the cell. The orientation of the decorated tubulin hooks is clockwise (arrow and inset). The plus end of the microtubules is toward the basal side of the cell. (B) The orientation of the decorated tubulin hooks is clockwise (inset). Bars: (A and B) 1  $\mu\text{m}$ ; (insets) 0.1  $\mu\text{m}$ .

**Table III. Microtubule Polarity Determined in Horizontal Sections**

Section site	Microtubules	Plus ends basal	Plus ends apical
	<i>n</i>	% ( <i>n</i> )	% ( <i>n</i> )
Basal	33	90.9 (30)	9.1 (3)
Middle	96	90.6 (87)	9.4 (9)
Apical	61	85.2 (52)	14.7 (9)

The microtubule polarity was determined in horizontal sections. Cross sections were made through the basal (below the nucleus), middle (nuclear), and apical (above the nucleus) regions. The hook orientation was counted in the micrographs.



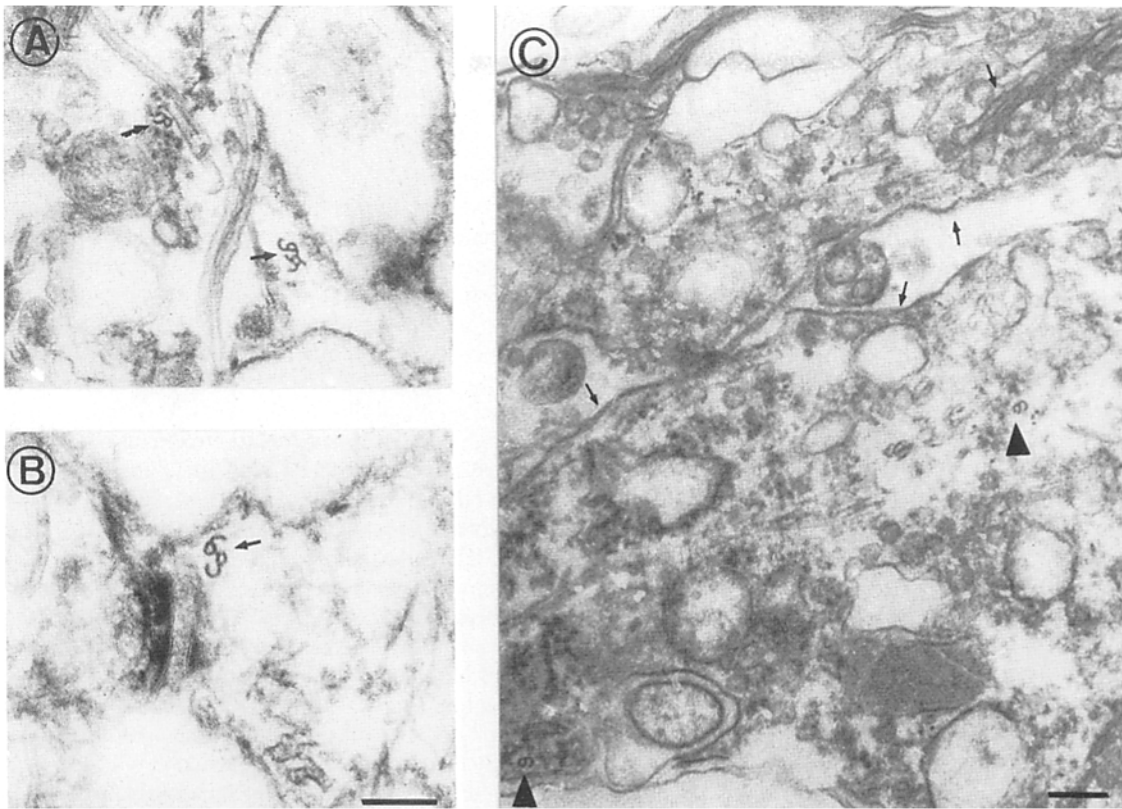


**Figure 6.** Polarity of the microtubules in the apical region. Horizontal sections. (A and B) Detergent-permeabilized cells. Microtubules perpendicular to the apical plane – i.e., longitudinal microtubules – have tubulin hooks oriented clockwise (arrows). The plus ends of these microtubules are toward the basal region of the cell. (C) Polarity of the microtubules in the apical web of electroporated cells. Tubulin was incorporated by electroporation. The Golgi complex and plasma membranes are well preserved (arrows). The polarity of the microtubules perpendicular to the section is plus end basal since the hooks are oriented clockwise (arrowheads). Bars: (A and B) 0.2  $\mu\text{m}$ ; (C) 0.2  $\mu\text{m}$ .

to examine the possible concomitant changes in Golgi organization and positioning. The change in Golgi complex localization was followed by double staining with an antibody directed against a peripheral membrane protein on the Golgi

membrane (Allen and Kreis, 1986) and anti-uvomorulin (Gumbiner and Simons, 1986) or anti-tubulin antibodies.

In isolated cells, examined 1 d after plating, the Golgi complex showed a compact organization and was located

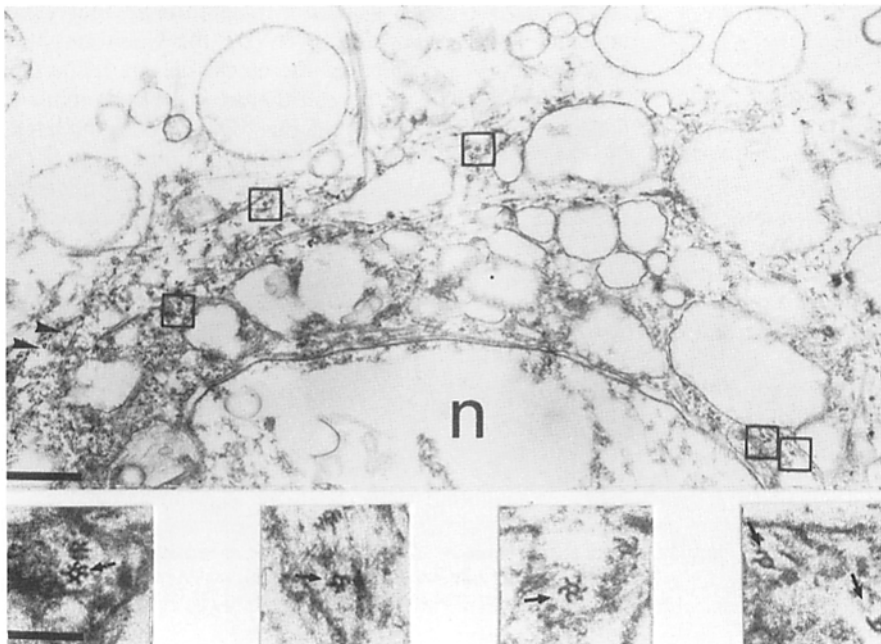


**Figure 7.** Polarity of the microtubules in the apical region. Vertical section of detergent-permeabilized cells. *n*, nucleus. The tubulin hooks are oriented counter-clockwise and clockwise with equal frequency. Insets are blown up images of the squared areas. Bars: (A and B) 1  $\mu\text{m}$ ; (insets) 0.2  $\mu\text{m}$ .

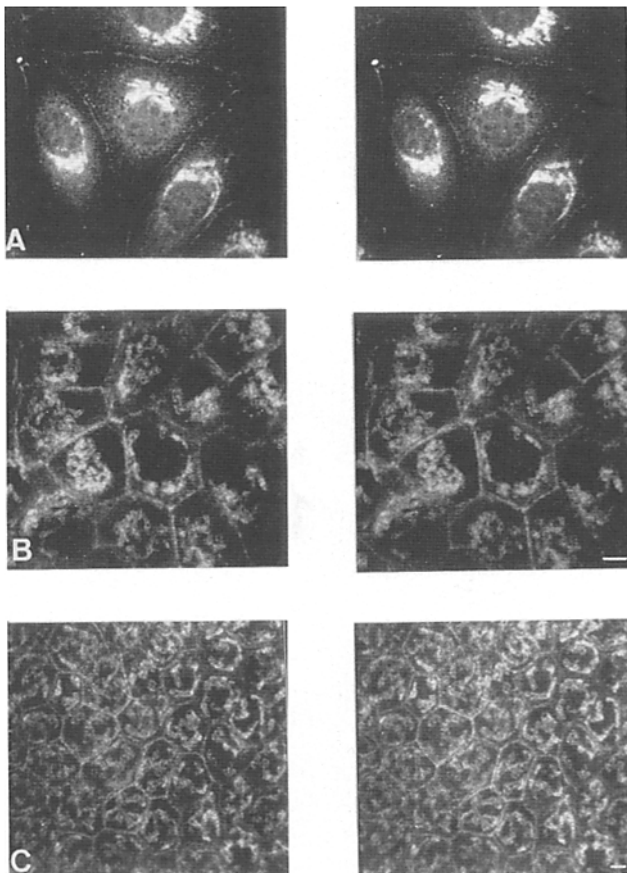


**Figure 8.** Stereo pair images of the Golgi complex and uvomorulin staining in MDCK cells. (A) 2 d after plating, the Golgi complex is contracted in a perinuclear location, although in some cells it has already begun to spread around the nucleus. Uvomorulin staining is found at the sites of cell-cell contacts and completely surrounds the cell. Transepithelial resistance is present at this stage. (B) 3 d after plating, the Golgi complex surrounds the nucleus and in some cases can be found in a more apical location. (C) The morphology of the Golgi complex in the final polarized, columnar state 5 d after plating. The Golgi complex has completed its apical migration. It extends as high as the uvomorulin staining. Bar, 5  $\mu$ m.

close to the nucleus around the two centrioles as observed in fibroblast cells. Most microtubules seemed to originate from this region (Fig. 1 B and Tables I and II). At this stage, uvomorulin and ZO-1 staining were observed intracellularly (data not shown).

2 d after plating, a transepithelial resistance developed, and a complete ring of ZO-1 protein (not shown) and uvomorulin staining delineated the cell contact sites (Fig. 8 A). In some cells, the Golgi complex began to spread around the nucleus. These cells appeared more fusiform and their microtubules did not radiate from the perinuclear area (Fig. 2 B). By 3 d, the cells began to show a polygonal shape, and the Golgi

complex was spread around the nucleus. In some cells, the Golgi complex began to migrate above the nucleus (Fig. 8 B). 5 d after plating, the diameter of the cells was drastically reduced, and the Golgi complex showed a convoluted tubular structure, reaching the level of the apical-most uvomorulin staining (Fig. 8 C) but not the level of the ZO-1 ring staining (data not shown).

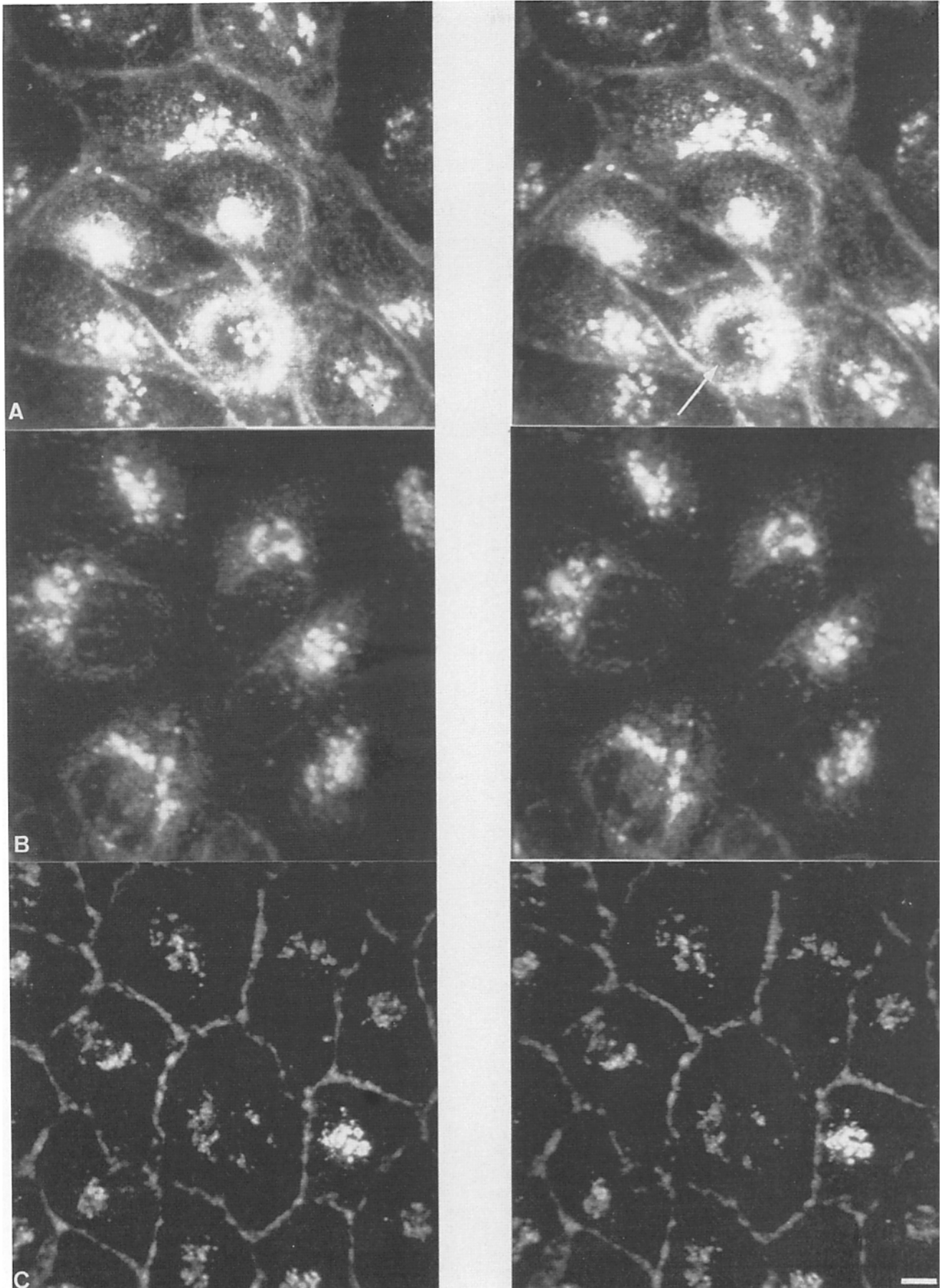
These observations showed that the Golgi complex changed from a compact structure located in the vicinity of the nucleus in isolated cells to a tubular complex located in the apical domain of fully polarized, columnar cells. Furthermore, the data suggested that spreading of the Golgi complex around the nucleus occurred after the establishment of tight junctions.

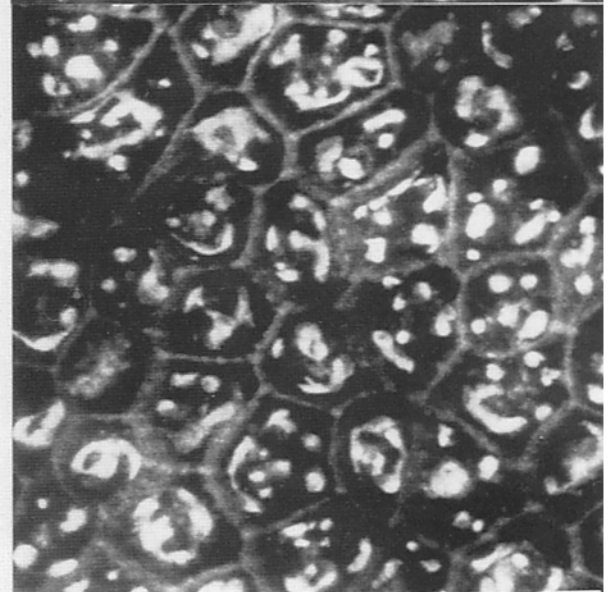
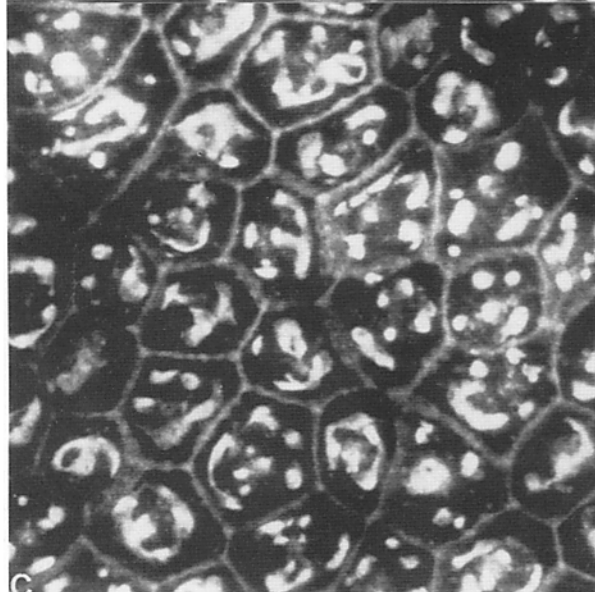
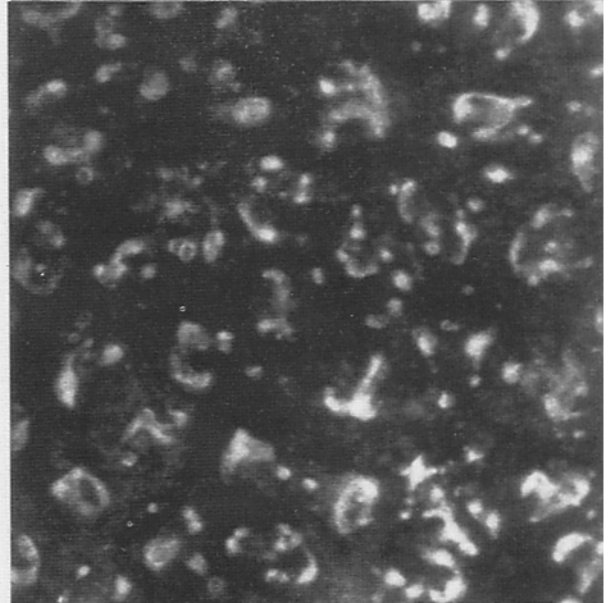
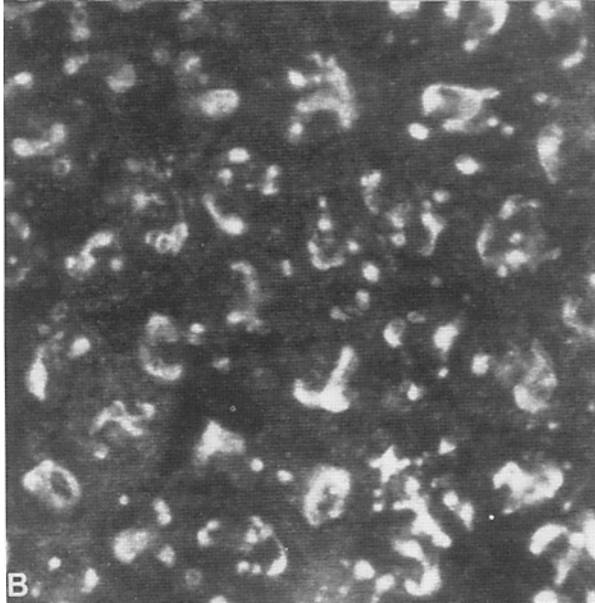
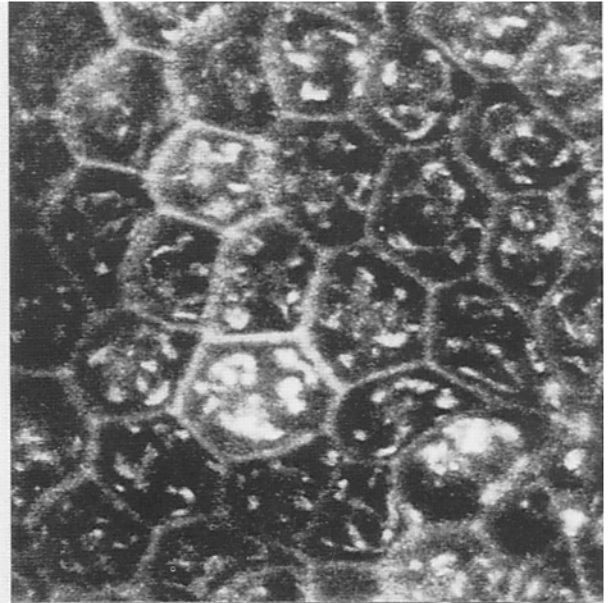
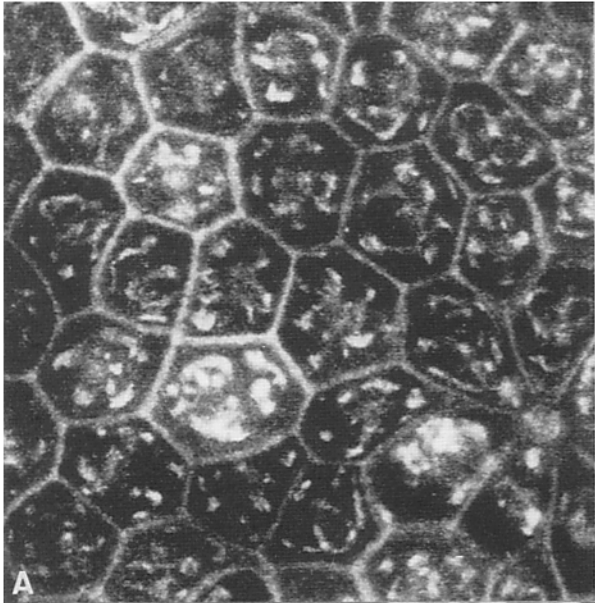
To examine the changes in Golgi morphology and compare the timing of Golgi movement with the formation of a tight monolayer, we labeled the cells with the fluorescent lipid analogue C6-NBD-ceramide (Lipsky and Pagano, 1985). This partially water-soluble lipid partitions into cells and accumulates in the Golgi complex after conversion into C6-NBD-sphingomyelin and glucosylceramide. These metabolic products move in vesicular carriers to the cell surface, where they are introduced into the exoplasmic leaflet of both the apical and basolateral plasma membranes (van Meer et al., 1987; Bennett et al., 1988). By this method, both the Golgi complex and the plasma membranes can be labeled simultaneously. Furthermore, back exchange with BSA can be used to determine when the tight junctions start to exert their fence function, obstructing lipid diffusion across the junction (van Meer et al., 1987). Using this assay, we determined whether the generation of a transepithelial resistance was correlated with the formation of the tight junction fence.

Incubation of isolated cells with C6-NBD-ceramide resulted in labeling of the Golgi complex and the cell surface (not shown). As expected from previous immunofluorescence data, the Golgi complex showed a compact organization and was located close to the nucleus. Adding BSA either to the apical or basal side of the cells removed all the surface staining (not shown). After 2 d of growth, the Golgi complex of cells labeled with C6-NBD-ceramide began to disperse in the cytoplasm (Fig. 9, A and B). In addition to Golgi staining, there was a "haziness" overlying the Golgi complex. This was due to staining of the apical plasma membrane dome. Adding BSA to the apical side of the cells removed the dome but not the linear staining, derived from the lateral membrane which was close to the substratum (Fig. 9 C). Conversely, adding BSA to the basal side of the filters removed the linear lateral staining but not the apical dome (Fig. 9 B). This showed that after 2 d of growth, when a transepithelial resistance started to develop, the fence for lipid diffusion was already operating.

In 5-d-old cells back exchange with BSA revealed the organization of the cell surface of the fully polarized cell. The apical back exchange removed the apical plasma membrane

**Figure 9.** Stereo pair images of plasma membrane and Golgi complex labeled with C6-NBD-ceramide 2 d after plating. (A) The apical and basolateral plasma membrane are labeled. The basolateral membrane forms the linear staining, while the apical membrane staining is seen as a hazy dome overlying the Golgi complex. The arrow shows a cell from which the apical cap was removed by the computer to expose the Golgi complex. (B) BSA back exchange of the basolateral membrane staining. The linear staining is removed and the apical membrane staining is intact. (C) BSA back exchange on the apical side. The linear staining is present and the overlying apical staining has been removed. More transport of C6-NBD-ceramide metabolites has occurred from the Golgi complex in these cells than in A and B. Bar, 5  $\mu$ m.





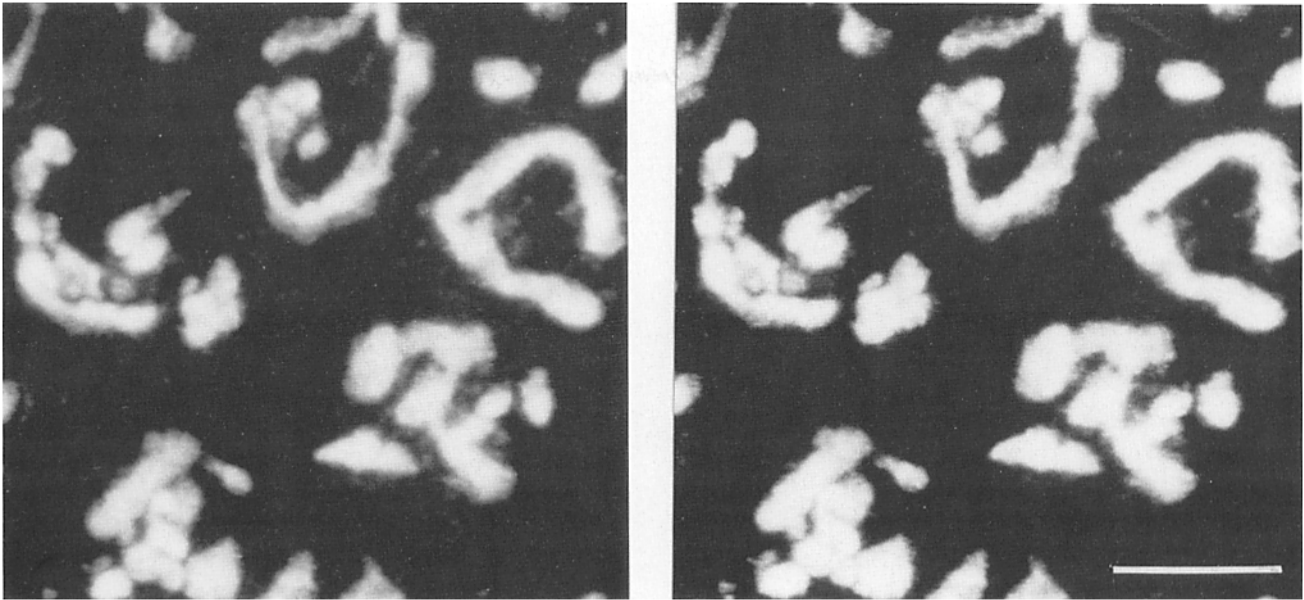


**Figure 11.** Stereo pair images of C6-NBD-ceramide labeling of the Golgi complex. The cells were labeled 5 d after plating. The Golgi complex forms a ribbon-like convoluted structure. Bar, 5  $\mu\text{m}$ .

staining (Fig. 10 C). Basal application of BSA completely removed the lateral staining of the cells up to the apical membrane (Fig. 10 B). The Golgi complex formed a ribbon-like convoluted structure in this final polarized state which had not been described before under cell culture conditions. Since the C6-NBD-ceramide studies had been performed after release from the 20°C block, it was possible that the entire Golgi structure was not visualized in these studies. To examine the entire Golgi morphology in the final polarized state, the cells were labeled with C6-NBD-ceramide at 37°C and incubated for 1 h at 20°C. Under these conditions, exit from the Golgi complex was blocked, and the Golgi morphology could be more completely examined. Fig. 11 shows that the Golgi complex formed a convoluted tubular structure. The overall morphology matches the morphology observed by immunofluorescence labeling using antibodies to Golgi-specific markers (Fig. 8 C and data not shown).

#### *Changes in Centriole Location during the Formation of a Columnar Epithelial Cell Monolayer*

Previous work has shown that in subconfluent MDCK strain II cells grown on glass the two centrioles are separated (Brè et al., 1987). In cells grown on polycarbonate filters, the centrosomes were found together in single cells 1 d after plating (Tables I and II). This was also the case in cells that had not developed extensive cell-cell contacts, as evidenced by staining for the ZO-1 protein along the perimeter of the cell (Siliaciano and Goodenough, 1988). In contrast, when the cells had developed a complete rim of ZO-1 protein, centrioles were found at a variable distance from each other. By day

5, the centrioles had moved back together and were observed in the same focal plane as the ZO-1 protein (Fig. 12). From this data and electron microscopy data, we conclude that the centrioles split and move apically during the establishment of epithelial cell polarity.

#### *Discussion*

Cells that form an epithelium in culture undergo a transition from the unpolarized to the polarized state every time that they are passaged. Our study analyzes the organizational changes in MDCK cells during the formation of a polarized monolayer. Within 12 h after plating, the majority of the isolated cells assume an organization in which the centrosome and the Golgi complex are located together in a region that appears to organize most of the microtubules. This is similar to what has been observed in fibroblasts (Singer and Kupfer, 1986). However, in these cells the microtubule-organizing material is more centered around the centrioles (Osborn and Weber, 1976).

2 d after plating, the MDCK cells reach confluency and the microtubules are not nucleated by a single microtubule-organizing complex any longer. The centrioles have split and the Golgi complex has moved around the nucleus. This occurs concomitantly with the establishment of cell junctions at the points of cell-cell contact along the cell perimeters as evidenced by the zonular assembly of uvomorulin and the ZO-1 protein. The tight junctions seem to be functional at this stage as evidenced by two different criteria. A trans-epithelial resistance develops and the fence function in the

**Figure 10.** Stereo pair images of plasma membrane and Golgi complex labeled with C6-NBD-ceramide 5 d after plating. (A) The apical and basolateral plasma membrane is labeled. The apical staining obscures the view of the Golgi complex, while the basolateral staining is columnar as compared with Fig. 9. (B) BSA back exchange of the basolateral membrane staining. The lateral pattern is removed. The apical membrane staining still partially obscures the Golgi staining. (C) BSA back exchange of the apical membrane staining. The Golgi can be seen more clearly, and the columnar basolateral staining is intact. Bar, 5  $\mu\text{m}$ .

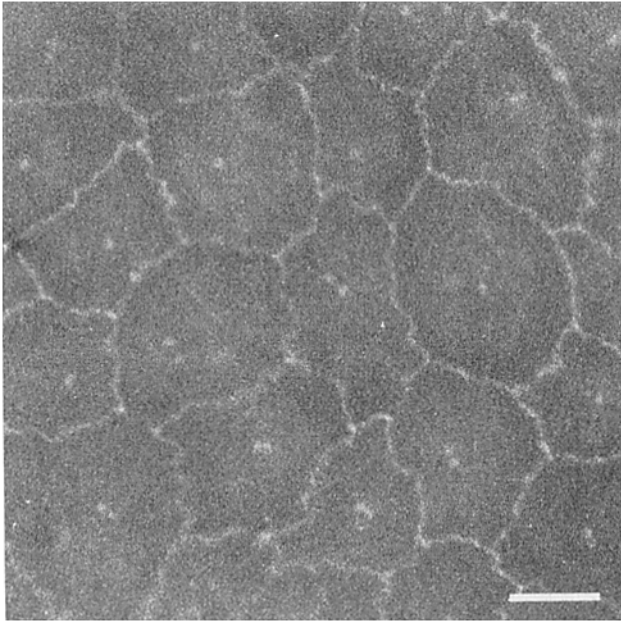


**Figure 12.** Centriole and ZO-1 protein staining in polarized columnar MDCK cells 5 d after plating. The cells were fixed and stained as described in Materials and Methods and viewed in the epifluorescence microscope. The punctate centrosome staining is in the same focal plane as the ZO-1 staining. Bar, 5  $\mu\text{m}$ .

exoplasmic leaflet of the plasma membrane bilayer operates as demonstrated by the back-exchange experiments using the C6-NBD-lipid marker. The development of cell surface polarity is known to continue after the tight junctions have been formed (Balcarova-Ständer et al., 1984; Herzlinger and Ojakian, 1984). Apical and basolateral components present on the wrong side of the fence have to be removed either by transcytosis to the correct domain or by degradation (Pesonen et al., 1984a,b; Cereijido et al., 1989).

Once a confluent monolayer is formed, the cells begin to change their shapes. The tight junctions that originally formed close to the substratum move upward  $>10 \mu\text{m}$  to circumscribe the apex of each columnar cell in the final "differentiated" state. This change in height is accompanied by a migration of the centrioles and the Golgi complex to the apical part of the cell. The final location of the two centrioles is in close apposition to the apical membrane where they do not nucleate many microtubules. Microtubule bundles have formed and these are parallel to the apical-basal axis of the cell. Determination of the polarity of these longitudinal microtubules by the hook method (Heidemann and McIntosh, 1980) showed that they are orientated with their plus ends basal. They seem to originate from sites located underneath the apical membrane. Longitudinal bundles running in the apical-basal direction have been observed previously in intestinal epithelium (Gorbisky and Borisy, 1985; Achler et al., 1989) as well as during the development of the neural tube in newt neurulation (Burnside, 1971). The newt neural epithelial cells are columnar cells of enormous height ( $\sim 100 \mu\text{m}$ ) and have long microtubules oriented from the apex to the base. Also, during *Drosophila* wing development, similar microtubular arrays are formed in the long axis of the epidermal cells (Tucker et al., 1986). The microtubules in these cells are not nucleated by centrosomes. Instead, they

are fixed to the plasma membrane on the apical and the basal sides by electron-dense attachment sites. The polarity of the microtubules is the same as we have found in MDCK cells (Mogensen et al., 1989). We have not identified the structures from which microtubules could be nucleated in the apical domain in MDCK cells. However, after treatment with cold and with nocodazole (nocodazole alone is not sufficient), the longitudinal bundles start depolymerizing from the basal side of the cell. Upon drug removal, the microtubules regrow from foci beneath the apical membrane (Bacallao, R., unpublished observation). This suggests that the microtubule-organizing foci are indeed located in the apical part of the cells. Recent studies using a monoclonal antibody against a 180-kD protein, localized in the pericentriolar area in many cell types, have shown that in MDCK cells the antigen spreads out upon establishment of cell-cell contacts (Buendia, B., M. Bornens, and E. Karsenti, unpublished observations). This antibody may allow the localization of the microtubule-organizing structures in polarized MDCK cells. Whether the plus ends of the microtubules remain free or are attached to basal structures as in *Drosophila* wing cells is not known. The resistance of microtubules to nocodazole treatment in columnar epithelial cells suggests that they are stabilized by specific microtubule-associated proteins and/or plus end-capping factors.

The Golgi complex undergoes a complex rearrangement in parallel with the development of the longitudinal microtubule arrays (Fig. 8-10). It starts spreading around the nucleus as the centrosome splits and then extends into the apical part of the cell. The final state of the Golgi complex in MDCK cells is reminiscent of the three-dimensional structure of the Golgi complex in Sertoli cells (Rambourg et al., 1979). In these cells, the Golgi complex forms a wavy ribbon- or plate-like structure that winds from the top of the nucleus to the apex of the cell. The studies of Rambourg et al. (1981, 1987) have demonstrated that there is only one interconnected Golgi complex in each cell type studied. Whether this is the case also for MDCK cells has to await an ultrastructural analysis. The "worm-like" structure of the MDCK Golgi complex is fragmented after microtubule depolymerization and disperses in the apical part of the cell (Bacallao, R., unpublished observations). Also, in other cell types, the structure of the Golgi complex is linked to microtubule organization (Thyberg and Moskalewski, 1985). In fibroblasts, the dispersed Golgi elements recluster after microtubule repolymerization from the microtubule-organizing complex (Rogalski and Singer, 1984). The Golgi elements move along microtubules towards their minus ends (Ho et al., 1989). Another example of Golgi movement during differentiation is observed when myoblasts fuse to form myotubes (Tassin et al. 1985a,b). The microtubule-nucleating activity changes from a centrosomal location to a circumnuclear distribution. Concomitantly, the Golgi complex spreads from its position around the centrosome in myoblasts to a location surrounding the nucleus in the myotubes. Apparently, the Golgi complex followed the movement of the pericentriolar material, dissociating from the centriole pair to form the circumnuclear microtubule-organizing complex.

It seems likely that the rearrangement of the Golgi complex during MDCK cell polarization is guided by the formation of the longitudinal microtubules. Since these do not focus on one microtubule-organizing center, the movement of

the interconnected Golgi complex along the microtubules towards their minus ends could explain the spread out and intertwined Golgi structure in the apical part of the cell. Thus, the microtubule network confers polarity to the cytoplasm. Our studies suggest that in MDCK cells the formation of cell-cell contacts is necessary to reorient cytoplasmic polarity from an arrangement similar to that seen in fibroblasts and other cell types to one that is unique for epithelial cells.

It is interesting to compare the morphogenesis of the MDCK cell epithelium with the process of forming an epithelium de novo from nonepithelial precursor cells. The trophectodermal cells in the developing mouse embryo have been extensively studied with markers similar to those used in this study (Fleming and Johnson, 1988). Up to the early eight-cell stage, the blastomere is organized in a symmetrical fashion except for the region of cell-cell contact. These intercellular interactions are mediated by ovomorulin (Vestweber et al., 1987) and lead to the establishment of the apical-basal axis. The cell surface polarizes and a basal pole is defined by contact to adjacent cells. The tight junction protein, ZO-1, is expressed at the eight-cell stage and is present at the boundary between the free and the apposed cell surface (Fleming et al., 1989). In a similar manner, the ZO-1 protein assembles at the edges of contacting MDCK cells. In the mouse embryo, the ZO-1 protein is initially organized in spots along the perimeter of the cells and assembles into zonular tight junctions at the 16-32-cell stage (Fleming et al., 1989). Exactly when the tight junction becomes functional and forms an occluding barrier between the cells as well as a molecular fence in the exoplasmic leaflet is not yet known. During the eight-cell stage, the microtubules redistribute to generate a highly concentrated meshwork underlying the developing apical pole. There is no centrosome at this stage, but pericentriolar material has been detected in the apical part of the cell using an autoantibody against human centrosomes (Houliston et al., 1987). However, in contrast to MDCK cells, the Golgi complex is located basally below the nucleus at the 16-cell stage. It is possible that the biosynthetic activity of the exocytic apparatus of the polarized trophoctoderm cell is directed towards the basal side into the developing blastocoel, and therefore the Golgi complex positions there as has been suggested to occur during corneal development. Trelstad (1970) has shown that the Golgi complex moves basally exactly at the time when the primary stroma and Bowman's membrane are assembled beneath the basolateral plasma membrane of the corneal epithelium.

The role of the microtubules in the polarized delivery of newly synthesized apical and basolateral proteins and lipids from the *trans*-Golgi network of MDCK cells has not yet been defined (Salas et al., 1986; Rindler et al., 1987). In other epithelial cells it seems likely that intact microtubules are necessary for facilitating delivery in the apical direction (Eilers et al., 1989; Achler et al., 1989). When microtubules are depolymerized by drugs, apical transport from the Golgi complex is decreased. Instead, apical proteins seem to be missorted in the basolateral direction. Apical carrier vesicles from the Golgi complex would have to be transported in the retrograde direction if the microtubular minus ends were apical. This is the opposite to the direction of polarized transport of cell surface proteins from the Golgi complex to the ruffling edge in fibroblasts. After microtubule depolymerization, polarized exocytosis in fibroblasts is abolished (Rogal-

ski et al., 1984). However, the rate of delivery to the unpolarized cell surface is unchanged or decreased by ~50% (Kääriäinen et al., 1980; Rogalski et al., 1984). It might very well be that transport to the basolateral surface is also facilitated by microtubules. Basolateral vesicular carriers could move to the basal side along microtubules. If this were the case, it is tempting to suggest that vesicular transport in the apical and in the basolateral directions occur with opposite polarity and with different motors (e.g., microtubule-associated protein 1C apically and kinesin basolaterally) (Paschal et al., 1987; Vale et al., 1985).

More work is obviously necessary to find out how exocytic traffic to the polarized cell surface is carried out in epithelial cells and to analyze the role of microtubules in generating and maintaining epithelial polarity. Our results on the organization of the microtubules and the Golgi complex in filter-grown MDCK cells show that this cell system should provide a useful experimental model for such studies.

The authors would like to thank Dr. Jan De May for helping to critically evaluate the fixation methods used. We also thank Hilikka Virta, Clemens Storz, and Bill Meir for their superb technical assistance. We would like to thank Drs. Michel Bornens, Jan De Mey, and Thomas Kreis for antibodies; Lawrence Livermore Laboratory for generously supplying the View image processing software; and Hank Lane for supplying Transwell filters. We are especially grateful to Dr. Kristian Prydz for his help in the electroporation of MDCK cells.

R. Bacallao is supported by a National Institutes of Health physician scientist award grant DK01777. C. Dotti is the recipient of an Alexander von Humboldt Stiftung fellowship.

Received for publication 15 June 1989 and in revised form 1 August 1989.

#### References

- Achler, C., D. Filmer, C. Merte, and D. Drenckhahn. 1989. Role of microtubules in polarized delivery of apical membrane proteins to the brush border of the intestinal epithelium. *J. Cell Biol.* 109:179-189.
- Allen, V., and T. E. Kreis. 1986. A microtubule-binding protein associated with the membranes of the Golgi apparatus. *J. Cell Biol.* 103:2229-2239.
- Balcarova-Ständer, J., S. E. Pfeiffer, S. D. Fuller, and K. Simons. 1984. Development of cell surface polarity in the epithelial Madin-Darby canine kidney (MDCK) cell line. *EMBO (Eur. Mol. Biol. Organ.) J.* 3:2687-2694.
- Bennett, M. K., A. Wandering-Ness, and K. Simons. 1988. Release of putative exocytic transport vesicles from perforated MDCK cells. *EMBO (Eur. Mol. Biol. Organ.) J.* 7:4075-4085.
- Berod, A., B. K. Hartman, and J. F. Pujol. 1981. Importance of fixation in immunohistochemistry: use of formaldehyde solutions at variable pH for the localization of tyrosine hydroxylase. *J. Histochem. Cytochem.* 29:844-850.
- Boller, K., D. Vestweber, and R. Kemler. 1985. Cell adhesion molecule ovomorulin is localized in the intermediate junctions of adult intestinal epithelial cells. *J. Cell Biol.* 100:327-332.
- Brè, M.-H., T. E. Kreis, and E. Karsenti. 1987. Control of microtubule nucleation and stability in Madin-Darby canine kidney cells: the occurrence of noncentrosomal, stable detyrosinated microtubules. *J. Cell Biol.* 105:1283-1296.
- Bornens, M., M. Paintrand, J. Berges, M. C. Marty, and E. Karsenti. 1987. Structural and chemical characterization of isolated centrosomes. *Cell Motil. Cytoskeleton.* 8:238-249.
- Burnside, B. 1971. Microtubules and microfilaments in newt neurulation. *Dev. Biol.* 26:416-441.
- Cajal, R. Y. 1914. Algunas variaciones fisiologicas y patologicas del aparato reticular de Golgi. *Trabajos del Laboratorio Cajal de Investigaciones Biologicas (Madrid).* 12:127.
- Cerejido, M., R. G. Contreras, and L. Gonzalez-Mariscal. 1989. Development and alteration of polarity. *Annu. Rev. Physiol.* 51:785-795.
- Ducibella, T., and E. Anderson. 1975. Cell shape and membrane changes in the eight-cell mouse embryo: prerequisites for morphogenesis of the blastocyst. *Dev. Biol.* 47:45-58.
- Dustin, P. 1978. Microtubules. Springer-Verlag New York Inc., New York. 452 pp.
- Eilers, U., J. Klumperman, and H.-P. Hauri. 1989. Nocodazole, a microtubule-active drug, interferes with apical protein delivery in cultured intestinal epithelial cells (Caco-2). *J. Cell Biol.* 108:13-22.
- Fleming, T. P., and M. H. Johnson. 1988. From egg to epithelium. *Annu. Rev.*

- Cell Biol.* 4:459-485.
- Fleming, T. P., J. McConnell, M. H. Johnson, and B. R. Stevenson. 1989. Development of tight junctions de novo in the mouse early embryo: control of assembly of the tight junction-specific protein, ZO-1. *J. Cell Biol.* 108:1407-1418.
- Gorbsky, G., and G. G. Borisy. 1985. Microtubule distribution in cultured cells and intact tissues: improved immunolabeling resolution through the use of reversible embedment cytochemistry. *Proc. Natl. Acad. Sci. USA.* 82:6889-6893.
- Griffiths, G., and K. Simons. 1986. The trans Golgi network: sorting at the exit site of the Golgi complex. *Science (Wash. DC).* 234:438-443.
- Gumbiner, B. 1987. Structure, biochemistry, and assembly of epithelial tight junctions. *Am. J. Physiol.* 22:749-758.
- Gumbiner, B., and K. Simons. 1986. A functional assay for proteins involved in establishing an epithelial occluding barrier: identification of a uvomorulin-like polypeptide. *J. Cell Biol.* 102:457-468.
- Gumbiner, B., B. Stevenson, and A. Grimaldi. 1988. The role of the cell adhesion molecule uvomorulin in the formation and maintenance of the epithelial junctional complex. *J. Cell Biol.* 107:1575-1587.
- Hay, E. D. 1982. Cell and extracellular matrix: their organization and mutual dependence. *Mod. Cell Biol.* 2:509-548.
- Heidemann, S. R., and J. R. McIntosh. 1980. Visualization of the structure polarity of microtubules. *Nature (Lond.).* 286:517-519.
- Herzlinger, D. A., and G. K. Ojakian. 1984. Studies on the development and maintenance of epithelial cell surface polarity with monoclonal antibodies. *J. Cell Biol.* 98:1777-1787.
- Ho, W. C., V. J. Allan, G. van Meer, E. G. Berger, and T. E. Kreis. 1989. Reclustering of scattered Golgi elements occurs along microtubules. *Eur. J. Cell Biol.* 48:250-263.
- Houliston, E., S. J. Pickering, and B. Maro. 1987. Redistribution of microtubules and pericentriolar material during the development of polarity in mouse blastomeres. *J. Cell Biol.* 104:1299-1308.
- Johnson, M. H., and B. Maro. 1985. A dissection of the mechanisms generating and stabilizing polarity in mouse 8- and 16-cell blastomeres: the role of cytoskeletal elements. *J. Embryol. Exp. Morph.* 90:311-334.
- Kääriäinen, L., K. Hashimoto, J. Saraste, I. Virtanen, and K. Penttinen. 1980. Monensin and FCCP inhibit the intracellular transport of alphavirus membrane glycoproteins. *J. Cell Biol.* 87:783-791.
- Klein, G., M. Langegger, R. Timpl, and P. Ekblom. 1988. Role of laminin A chain and the development of epithelial cell polarity. *Cell.* 55:331-341.
- Kronebusch, P. J., and S. J. Singer. 1987. The microtubule-organizing complex and the Golgi apparatus co-localized around the entire nuclear envelope of interphase cardiac myocytes. *J. Cell Sci.* 88:25-34.
- Kupfer, A., S. J. Singer, and G. Dennert. 1986. On the mechanism of unidirectional killing in mixtures of two cytotoxic T lymphocytes: unidirectional polarization of cytoplasmic organelles and the membrane-associated cytoskeleton in the effector cell. *J. Exp. Med.* 163:489-498.
- Lipsky, N., and R. E. Pagano. 1985. Intracellular translocation of fluorescent sphingolipids in cultured fibroblasts: endogenously synthesized sphingomyelin and glucocerebroside analogues pass through the Golgi apparatus en route to the plasma membrane. *J. Cell Biol.* 100:27-34.
- Mitchison, T. J., and M. W. Kirschner. 1984. Microtubule assembly nucleated by isolated centrosomes. *Nature (Lond.).* 312:232-236.
- Mogensen, M. M., J. B. Tucker, and H. Stebbings. 1989. Microtubule polarities indicate that nucleation and capture of microtubules occurs at cell surfaces in *Drosophila*. *J. Cell Biol.* 108:1445-1452.
- Osborn, M., and K. Weber. 1976. Cytoplasmic microtubules in tissue culture cells appear to grow from an organizing structure towards the plasma membrane. *Proc. Natl. Acad. Sci. USA.* 73:867-871.
- Paschal, B. M., H. S. Shpetner, and R. B. Vallee. 1987. MAP 1C is a microtubule-activated ATPase which translocates in vitro and has dynein-like properties. *J. Cell Biol.* 105:1273-1282.
- Pesonen, M., W. Ansoorge, and K. Simons. 1984a. Transcytosis of the G protein of vesicular stomatitis virus after implantation into the apical plasma membrane of Madin-Darby canine kidney cells. I. Involvement of endosomes and lysosomes. *J. Cell Biol.* 99:796-802.
- Pesonen, M., R. Bravo, and K. Simons. 1984b. Transcytosis of the G protein of vesicular stomatitis virus after implantation into the apical membrane of Madin-Darby canine kidney cells. II. Involvement of the Golgi complex. *J. Cell Biol.* 99:803-809.
- Quaroni, A., K. Kirsch, and M. A. Weiser. 1979. Effect of colchicine on the redistribution of L-[1,5,6-<sup>3</sup>H]fucose-labelled membrane glycoproteins among Golgi, lateral basal and microvillus membranes. *Biochem. J.* 182:213-221.
- Rambourg, A., Y. Clermont, and L. Hermo. 1979. Three-dimensional architecture of the Golgi apparatus in sertoli cells of the rat. *Am. J. Anat.* 154:455-476.
- Rambourg, A., Y. Clermont, and L. Hermo. 1981. Three-dimensional structure of the Golgi apparatus. *Methods Cell Biol.* 23:155-166.
- Rambourg, A., Y. Clermont, L. Hermo, and D. Segretain. 1987. Three-dimensional structure of the Golgi apparatus of nonciliated epithelial cells of the ductuli efferentes in rat: an electron microscope stereoscopic study. *Biol. Cell.* 60:103-116.
- Rindler, M. J., I. E. Ivanov, and D. D. Sabatini. 1987. Microtubule-acting drugs lead to the nonpolarized delivery of the influenza hemagglutinin to the cell surface of polarized Madin-Darby canine kidney cells. *J. Cell Biol.* 104:231-241.
- Rodriguez-Boulant, E., K. T. Paskiet, and D. D. Sabatini. 1983. Assembly of enveloped viruses in Madin-Darby canine kidney cells: polarized budding from single attached cells and from clusters of cells in suspension. *J. Cell Biol.* 96:866-874.
- Rogalski, A. A., and S. J. Singer. 1984. Association of the Golgi apparatus with microtubules. *J. Cell Biol.* 99:1092-1100.
- Rogalski, A. A., J. E. Bergmann, and S. J. Singer. 1984. Effect of microtubule assembly status on the intracellular processing and surface expression of an integral protein of the plasma membrane. *J. Cell Biol.* 99:1101-1109.
- Roth, K. E., C. L. Rieder, and S. S. Bowser. 1988. Flexible-substratum technique for viewing cells from the side: some in vivo properties of primary (9 + 0) cilia in cultured kidney epithelia. *J. Cell Sci.* 89:457-466.
- Salas, P. J. I., D. E. Misk, D. E. Vega-Salas, D. Gundersen, M. Cerijido, and E. Rodriguez-Boulant. 1986. Microtubules and actin filaments are not critically involved in the biogenesis of epithelial cell surface polarity. *J. Cell Biol.* 102:1853-1867.
- Siliciano, J. D. A., and D. A. Goodenough. 1988. Localization of the tight junction protein, ZO-1, is modulated by extracellular calcium and cell-cell contact in Madin-Darby canine kidney epithelial cells. *J. Cell Biol.* 107:2389-2399.
- Singer, S. J., and A. Kupfer. 1986. The directed migration of eukaryotic cells. *Annu. Rev. Cell Biol.* 2:337-365.
- Stelzer, E. H. K., R. Stricker, R. Pick, C. Storz, and P. Hänninen. 1989. Confocal fluorescence microscopes for biological research. In Scanning Imaging. *Proc. Soc. Photo-opt. Instrum. Eng., Bellingham, WA.* Tony Wilson, editor. 146-151.
- Stevenson, B. R., J. D. Siliciano, M. S. Mooseker, and D. A. Goodenough. 1986. Identification of ZO-1: a high molecular weight polypeptide associated with the tight junction (zonula occludens) in a variety of epithelia. *J. Cell Biol.* 103:755-766.
- Tassin, A.-M., B. Maro, and M. Bornens. 1985a. Fate of microtubule-organizing centers during myogenesis in vitro. *J. Cell Biol.* 100:35-46.
- Tassin, A.-M., M. Paintrand, E. G. Berger, and M. Bornens. 1985b. The Golgi apparatus remains associated with microtubule organizing centers during myogenesis. *J. Cell Biol.* 101:630-638.
- Thyberg, J., and S. Moskalewski. 1985. Microtubules and the organization of the Golgi complex. *Exp. Cell Res.* 159:1-16.
- Trelstad, R. L. 1970. The Golgi apparatus in chick corneal epithelium: changes in intracellular position during development. *J. Cell Biol.* 45:34-42.
- Tucker, J. B., M. J. Milner, D. A. Currie, J. A. Muir, D. A. Forrest, and M. J. Spencer. 1986. Centrosomal microtubule organizing centers and a switch in the control of protofilament number for cell surface-associated microtubules during *Drosophila* wing morphogenesis. *Eur. J. Cell Biol.* 41:279-289.
- Vale, R. D., T. S. Reese, and M. P. Scheetz. 1985. Identification of a novel force-generating protein, kinesin, involved in microtubule-based motility. *Cell.* 42:39-50.
- van Meer, G., E. H. K. Stelzer, R. W. Wijnaendts-van-Resandt, and K. Simons. 1987. Sorting of sphingolipids in epithelial (Madin-Darby canine kidney) cells. *J. Cell Biol.* 105:1623-1635.
- Vega-Salas, B. E., P. J. I. Salas, D. Gundersen, and E. Rodriguez-Boulant. 1987. Formation of the apical pole of epithelial (Madin-Darby canine kidney) cells: polarity of an apical protein is independent of tight junctions while segregation of a basolateral marker requires cell-cell interactions. *J. Cell Biol.* 104:905-916.
- Vestweber, D., A. Gossler, K. Boller, and R. Kemler. 1987. Expression and distribution of cell adhesion molecule uvomorulin in mouse preimplantation embryos. *Dev. Biol.* 124:451-456.
- Wandinger-Ness, A., and K. Simons. 1989. The polarized transport of surface proteins and lipids in epithelial cells. In *Intracellular Trafficking of Proteins*. J. Hanover and C. Stern, editors. Cambridge University Press, Cambridge. In press.